Frequency and Polarizing Magnetic Field Dependence of the Clausius-Mossotti Factor of a Kerosene-Based Ferrofluid with Mn-Fe Nanoparticles in a Microwave Field

Iosif Malaescu *, Paul C. Fannin, Catalin N. Marin *, Ioana Marin, Corneluta Fira-Mladinescu

Posted Date: 26 February 2026

doi: 10.20944/preprints202602.1309.v1

Keywords: ferrofluid; dielectric permittivity; Clausius-Mossotti factor

 doi:10.20944/preprints202602.1309.v1

Article

Frequency and Polarizing Magnetic Field Dependence of the Clausius-Mossotti Factor of a Kerosene-Based Ferrofluid with Mn-Fe Nanoparticles in a Microwave Field

Iosif Malaescu [1,2], Paul C. Fannin [3], Catalin N. Marin [1,4,*], Ioana Marin [4,5] and Corneluta Fira-Mladinescu [4,5]

[1] Department of Physics, West University of Timisoara, Bd. V. Parvan no. 4, 300223 Timisoara, Romania
[2] Institute for Advanced Environmental Research, West University of Timisoara (ICAM - WUT), Oituz Str., No. 4, 300086 Timisoara, Romania
[3] Department of Electronic and Electrical Engineering, Trinity College, The University of Dublin, Dublin 2, Ireland
[4] Center for Studies in Preventive Medicine, "Victor Babes" University of Medicine and Pharmacy, 300041, Timisoara, Romania
[5] Department of Microbiology, Discipline of Hygiene, "Victor Babes" University of Medicine and Pharmacy, 300041, Timisoara, Romania
* Correspondence: catalin.marin@e-uvt.ro

Abstract

We present frequency- and magnetic field-dependent measurements of the complex dielectric permittivity ε*(f, H) of a kerosene-based ferrofluid, containing $Mn_{0.6}Fe_{0.4}Fe_2O_4$ nanoparticles, over 0.8–5 GHz and static fields up to ~91 kA/m. The imaginary part, ε''_F, shows a peak at a characteristic frequency that shifts towards higher frequencies with increasing H, revealing a magnetic field-dependent relaxation process, interpreted using the Maxwell–Wagner–Sillars model. Dielectrophoretic extraction of nanoparticles was evaluated via the squared electric field gradient, and a threshold, $\left(\nabla E^2\right)_{\min}$, dependent on particle size was determined. Below that threshold, Brownian forces dominate, so the ferrofluid acts as a homogeneous dielectric. For this case, the Clausius-Mossotti factor (CM) was calculated for ferrofluid droplets in air and in water as a function of frequency and magnetic field. In air, CM exhibits modest but systematic magnetic field dependence, indicating magnetically modulated dielectric response at GHz frequencies. In contrast, when water is used as the reference medium, CM remains negative and essentially independent of H across the entire frequency range, suggesting that the high permittivity of water masks magneto-dielectric effects in the ferrofluid. These findings provide insight into the interplay between magnetic field and permittivity of ferrofluids, with implications for high-frequency applications. Moreover, using a $\lambda/4$ antenna connected to a network analyzer, the existence of the dielectrophoretic force acting on a ferrofluid-impregnated textile thread, at microwave frequencies, was experimentally demonstrated.

Keywords: ferrofluid; dielectric permittivity; Clausius-Mossotti factor

1. Introduction

Ferrofluids are defined as stable colloidal systems of magnetic single-domain nanoparticles dispersed in a carrier liquid and stabilized by a surfactant coating to prevent agglomeration [1,2]. Ferrofluids exhibit both static and dynamic magnetic and dielectric properties, which are exploited in numerous technological [3,4] and biomedical [5,6] applications.

 doi:10.20944/preprints202602.1309.v1

Dielectrophoresis is a phenomenon in which polarizable particles experience a force when subjected to a non-uniform electric field [7]. This force arises from the interaction between the particle's dipole moment and the electric field gradient, causing particles to move toward regions of higher or lower field intensity, depending on their dielectric properties relative to the surrounding medium [7]. Due to its ability to manipulate particles without requiring labels or direct contact, dielectrophoresis has become a powerful tool in microfluidics [8], with applications in particle separation [9], characterization [10], and biomedical diagnostics [11].

Dielectrophoresis (DEP) can be classified based on the frequency of the applied electric field, which strongly influences particle response. Low-frequency DEP (< 1 MHz) primarily exploits particle conductivity and double-layer effects, making it ideal for manipulating cells and bacteria [12,13]. Radiofrequency DEP (1–100 MHz) probes both dielectric and conductive properties, enabling the selective separation of cells based on physiological differences [14,15]. Microwave DEP (> 100 MHz) targets dielectric relaxation of nanoparticles and subcellular structures, allowing manipulation and characterization of viruses, exosomes, and other nanoscale particles [16–18].

Overall, the choice of frequency enables the tailoring of DEP for specific particle types and applications, ranging from bulk cell separation to nanoscale particle characterization, providing versatile tools for biomedical, analytical, and nanotechnology research.

Applying dielectrophoresis to ferrofluids allows for the controlled reorganization and structuring of suspended magnetic nanoparticles, ferrofluid droplets, enabling the creation of tunable or "smart" fluid materials with customized physical properties. Additionally, this method permits selective separation or detailed characterization of nanoparticles based on their dielectric response. By combining dielectrophoretic manipulation with magnetic fields, it becomes possible to achieve both electrical and magnetic control within a single system, providing versatile options for microfluidic, sensing, and adaptive material applications.

This study seeks to investigate the frequency and static magnetic field-dependent behavior of the Clausius-Mossotti factor of a ferrofluid containing manganese ferrite nanoparticles, within the frequency range of 0.8–5 GHz and under magnetic field strengths ranging from 0 to approximately 91 kA/m. The objective of this study is to evaluate the feasibility of the dielectrophoresis phenomenon of ferrofluids at microwave frequencies, bearing in mind possible technical or biomedical applications.

2. Materials and Methods

The sample used for the measurements was a kerosene-based ferrofluid, containing mixed ferrite particles of the $Mn_xFe_{1-x}Fe_2O_4$ type (with x=0.6), having a density ϱ_F = 1.11 g/cm^3. It was obtained by chemical coprecipitation in aqueous solution of bivalent and trivalent iron salts with an excess of NH_4OH; the expected composition resulted from the use of the following raw materials: $MnSO_4 \cdot 4H_2O$ (0.6 mol), $FeSO_4 \cdot 7H_2O$ (0.4 mol), $FeCl_3$ with excess NH_4OH [19,20]. The stabilization of the obtained mixed Mn-Fe ferrite particles was achieved by hydrophobization with oleic acid in the absence of the dispersion medium (kerosene) by heat treatment at 97 °C for 1.5 hours [20], followed by filtration in an aqueous medium to purify the obtained phase. Finally, the resulting magnetic material was dispersed in kerosene, and to remove traces of water, a slight heating above 100 °C was performed, followed by magnetic field gradient filtration to eliminate clusters and large particles [20,21].

Using an inductive method [22], the dependence of the magnetization, M, on the magnetic field, H (Figure 1), of the investigated ferrofluid sample, at room temperature, was determined, resulting in a Langevin-type magnetization curve [1].

 doi:10.20944/preprints202602.1309.v1

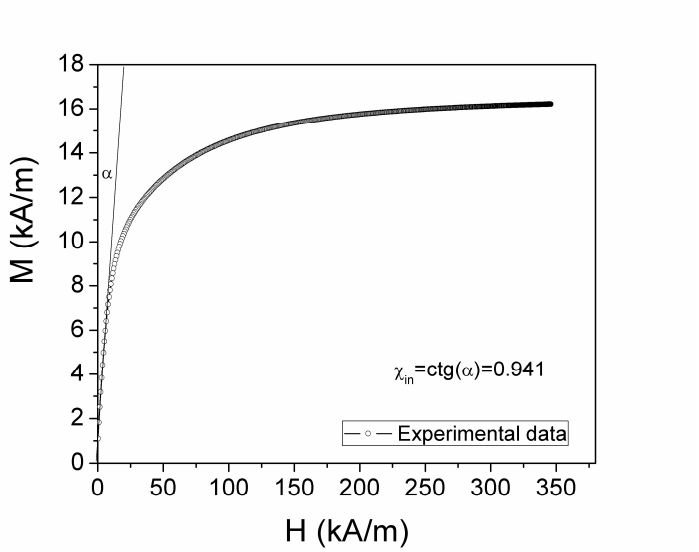

Figure 1. Magnetization curve of the investigated ferrofluid sample.

Based on the magneto-granulometric analysis [23] and static magnetization curve M(H) from Figure 1, assuming a spherical shape of the particles, the saturation magnetization of ferrofluid (M_{sat}), the mean magnetic diameter of particles (d_m), the particle concentration (n), and the initial susceptibility (χ_{in}) were determined. The following values were obtained: M_{sat} = 16.2 kA/m; d_m = 13.42 nm; n = $4.41 \cdot 10^{22}$ m^{-3} and χ_{in} = 0.941.

The complex dielectric permittivity, ε(f, H), of the sample was measured using the open-circuited (OC) coaxial transmission line technique [24,25], over the frequency range (f), between 0.8 GHz and 5 GHz, and at different values of static magnetic field (H), between 0 and approximately 91 kA/m. For this, an HP 8753C network analyzer [25] was used with a 50 Ω Hewlett-Packard coaxial line, including a coaxial cell containing the ferrofluid sample. The coaxial cell was placed between the poles of an electromagnet, with the cell axis perpendicular to the magnetic field.

For the experiment that proves the existence of the microwave dielectrophoretic force, we used a λ/4 antenna, connected with a 50 Ω coaxial cable to an Agilent FieldFox network analyzer, type N9923A.

3. Results and Discussion

The dielectrophoretic force acting on an entity (particle, cell, droplet, etc.) suspended in a medium with complex dielectric permittivity, ε_m^*, is given by the relationship:

$$F_{DEP} = 2\pi r^3 \varepsilon_0 \varepsilon'_m \,\mathrm{Re}\left[K^*(\omega)\right] \nabla E^2 \tag{1}$$

In relation (1), r is the radius of the entity (assumed of spherical shape), ε_0, is the dielectric permittivity of vacuum, ε'_m, is the real component of the relative complex dielectric permittivity of the entity, ω = 2πf is the angular frequency, E is the amplitude of the electric field, and K*(ω) is the complex Clausius-Mossotti factor,

$$K^*(\omega) = \frac{\varepsilon_p^*(\omega) - \varepsilon_m^*(\omega)}{\varepsilon_p^*(\omega) + 2\varepsilon_m^*(\omega)} \tag{2}$$

 doi:10.20944/preprints202602.1309.v1

In equation (2), $\varepsilon_p^*(\omega)$ is the complex dielectric permittivity of the entity (particle, cell, droplet, etc.), and $\varepsilon_m^*(\omega)$ is the complex dielectric permittivity of the environment in which the entity is located.

3.1. Clausius-Mossotti Factor of the Nanoparticles in Ferrofluid

Before addressing any aspects of the dielectrophoretic behavior of a ferrofluid (or colloidal systems in general), it is essential to evaluate the dielectrophoretic force acting on an individual particle suspended in the carrier liquid. Such an analysis allows one to determine whether the ferrofluid responds to an electric field gradient as a homogeneous medium, or whether particle agglomeration occurs, potentially leading to local inhomogeneity or even to phase separation between the solid particles and the carrier liquid, as a result of the dielectroforetic force action on nanoparticles within the ferrofluid.

Let us consider a manganese ferrite nanoparticle with a typical radius for nanoparticles in a ferrofluid, r = 5 nm [1], suspended in kerosene ($\varepsilon'_m \approx 2$). The relative dielectric permittivity of manganese ferrite is on the order of hundreds at low frequencies, and decreases to values on the order of tens at frequencies around the kilohertz range [26].

When the particle permittivity is very high, the real part of the Clausius–Mossotti factor approaches unity. In the case of micro- or nano-electrodes, extremely high electric field gradients can be achieved (such as $\nabla E^2 \approx 10^{17}\, V^2/m^3$ in the reference [27]), and assuming the idealized maximum value of Re[K*] = 1, the resulting dielectrophoretic force for this field gradient is approximately 1.4 × 10^{-18} N.

The Brownian force can be estimated using equation (3) [28], based on the assumption that the thermal energy k_BT is at least equal to the mechanical work required to displace the particle by a distance corresponding to its radius. Therefore, at room temperature (T = 300 K), one gets $F_B = 8 \cdot 10^{-13}\, N$.

$$F_B \approx \frac{k_B T}{r} \tag{3}$$

By comparing the dielectrophoretic force, which acts on a nanoparticle, with the Brownian force, it results that an electric field gradient, $\nabla E^2 \approx 10^{17}\, V^2/m^3$ (as in reference [27]) cannot produce agglomerations of nanoparticles in a ferrofluid, and its homogeneity cannot be affected by the dielectroforetic force.

For a particle with the radius, r, located in kerosene ($\varepsilon'_m \approx 2$), and for the idealized maximum limit, Re[K*] = 1, from equations (2) and (3), it follows that for the dielectrophoretic force to be greater than the Brownian force, at room temperature, the squared electric field gradient should fulfill the condition:

$$\nabla E^2 \geq \frac{k_B T}{2\pi r^4 \varepsilon_0 \varepsilon'_m \operatorname{Re}\left[K^*\right]} = \left(\nabla E^2\right)_{\min} \tag{4}$$

Figure 2 shows the theoretical dependence of $\left(\nabla E^2\right)_{\min}$ on the radius of a manganese ferrite particle in kerosene, computed at room temperature and under the assumption of idealized maximum limit, Re[K*] = 1. This figure delineates the range of the squared electric field gradient, ∇E^2, values for which the dielectrophoretic force, F_{DEP} acting on a particle of radius, r, surpasses the Brownian force acting on the same particle, F_B. Also, from Figure 2, it can be seen that nanoparticle aggregates could be extracted from the ferrofluid, under practically achievable field gradient conditions.

 doi:10.20944/preprints202602.1309.v1

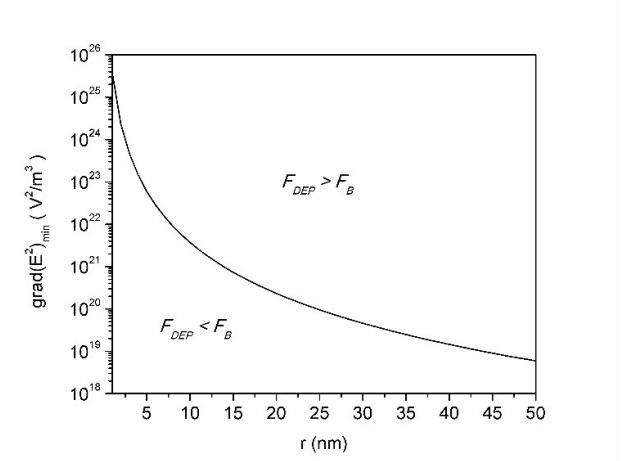

Figure 2. Theoretical dependence of $\left(\nabla E^2\right)_{\min}$ on the radius of a manganese ferrite particle in kerosene.

For non-aggregated nanoparticles, which have a typical radius, r = 5 nm, located in kerosene ($\varepsilon'_m \approx 2$), it follows that for the dielectrophoretic force to be greater than the Brownian force, at room temperature, the squared electric field gradient should be $\nabla E^2 \geq 6 \cdot 10^{22}\, V^2 / m^3$. Such a gradient value is very high and can be obtained with nano-tips, which have gaps between them of the order of tens of nanometers at most, but also, a possible achievement through e-beam lithography [29].

Otherwise, with thicker electrodes and a larger distance between them, the ferrofluid behaves as a homogeneous system, in the absence of other factors that would spoil the local homogeneity, because the dielectrophoretic force is smaller than the Brownian force acting on the individual nanoparticles dispersed in the carrier liquid of the ferrofluid. Under these conditions, the effective dielectric permittivity of the ferrofluid, as a homogeneous sample, is significant for dielectrophoresis experiments with ferrofluids.

3.2. Frequency and Magnetic Field Dependence of the Dielectric Permittivity of Ferrofluid

Figure 3 shows the experimental frequency dependence of the components ε'_F and ε''_F of the complex dielectric permittivity over the frequency range (0.8 - 5) GHz for different values of the magnetic field, H, ranging from 0 to 91 kA/m.

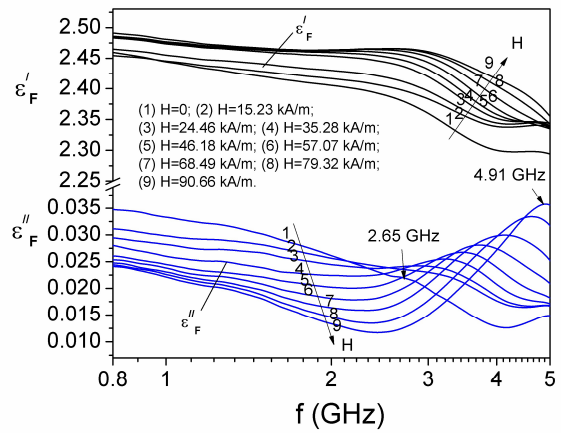

Figure 3. The frequency dependence of components of the complex dielectric permittivity at different values, H, of the magnetic field.

 doi:10.20944/preprints202602.1309.v1

From Figure 3, it is observed that for a constant value, H, of the magnetic field, the real component ε'_F decreases over the entire frequency range from 0.8 GHz to 5 GHz, whilst for a constant frequency f, the component ε'_F gradually increases with increasing field H.

Regarding the variation with frequency of ε''_F, it is observed that within the range (0.8 – 2) GHz, it gradually decreases with increasing field H, after which within the range (2.5 - 5) GHz, ε''_F exhibits both increases and decreases with increasing H. Also, from Figure 3, it is observed that the component ε''_F shows a maximum at a frequency f_{max} that moves from 2.65 GHz to 4.70 GHz with increasing H from 0 to 90.66 kA/m, which indicates the existence of a dielectric relaxation process, correlated with the polarization of the ferrofluid particles in the presence of the electric microwave field. This relaxation process corresponds to the Maxwell-Wagner-Sillars polarization phenomenon, also known as interfacial polarization [30,31]. Such behavior of the ε'_F and ε''_F components is influenced by the shape of the particles and the orientation of the electric dipoles in the direction of the electric field [30,31], as well as by the particle agglomerations induced by the magnetic field. At the same time, the electric dipole moment of the particles in the presence of the magnetic field changes compared to the electric dipole moment of the particles in the absence of the magnetic field, which will determine the increase or decrease of the components of the complex dielectric permittivity in different frequency or magnetic field domains [31] (see Figure 3).

A theoretical explanation of the frequency and static magnetic field dependence of the complex dielectric permittivity can be made based on the theoretical model in reference [31]. In this theoretical model [31], a colloidal system consisting of magnetic ellipsoids dispersed in a liquid medium is considered, and the dielectric permittivity of the system is given by the Maxwell-Wagner-Sillars model.

The analysis of the theoretical dependencies of ε'_F and ε''_F shows that an increase in the eccentricity of the ellipsoids leads to an increase in the permittivity, ε'_F, of the colloidal system, and an increase in the electrical conductivity of the ellipsoids leads to a shift of the maximum of ε''_F towards higher frequencies.

In the case of ferrofluids, the agglomeration of magnetic nanoparticles into small aggregates, formed by several particles (which behave in the carrier liquid as a large particle) can be done under the action of a static magnetic field applied to the ferrofluid. On the other hand, through the magnetoresistive tunneling effect, the electrical resistance between two magnetic particles decreases as their magnetic moments align. Thus, by applying a magnetic field, the occurrence of aggregates of a few particles is equivalent to increasing the eccentricity of the particles in the colloidal system. At the same time, the electrical conductivity of such an aggregate increases through the tunnel magnetoresistive effect. So, the increase in the real component of the permittivity, ε'_F, and the shift to higher frequencies of the maximum of ε''_F with increase in magnetic field (as seen in Figure 3) is due to the formation of nanoparticle aggregates in the ferrofluid, as well as to the tunnel magnetoresistive effect inside such an aggregate of a few nanoparticles.

3.3. Clausius-Mossotti Factor of the Ferrofluid in Air

The Clausius-Mossotti complex factor for a droplet of ferrofluid in air is:

$$K_{FA} = \frac{\varepsilon_F^* - 1}{\varepsilon_F^* + 2} \tag{5}$$

Using the complex form for the dielectric permittivity of ferrofluid, after performing some calculations, the expressions of the real (K'_{FA}) and imaginary (K''_{FA}) components of the Clausius-Mossotti complex factor result in:

 doi:10.20944/preprints202602.1309.v1

$$K'_{FA} = \frac{\varepsilon'_F{}^2 + \varepsilon''_F{}^2 + \varepsilon'_F - 2}{\varepsilon'_F{}^2 + \varepsilon''_F{}^2 + 4\varepsilon'_F + 4} \tag{6}$$

$$K''_{FA} = \frac{3\varepsilon''_F}{\varepsilon'_F{}^2 + \varepsilon''_F{}^2 + 4\varepsilon'_F + 4} \tag{7}$$

Using the experimental values of ε'_F and ε''_F, from Figure 3, by means of equations (6) and (7), the K'FA and K''FA components of the Clausius-Mossotti complex factor were determined. Their frequency and magnetic field dependence are shown in Figure 4. From Figure 4, it can be observed that the frequency dependence of the K'FA and K''FA components of the Clausius–Mossotti complex factor is similar to the dependencies of the components of the complex dielectric permittivity from Figure 3. Since air has a relative dielectric permittivity equal to unity, variations in the Clausius-Mossotti factor are directly related to changes in the permittivity of the ferrofluid itself. It is also observed from Figure 4 that Re[KFA] is positive; therefore, the dielectrophoretic force is positive, and the ferrofluid droplet located in air is attracted toward regions of higher electric field intensity.

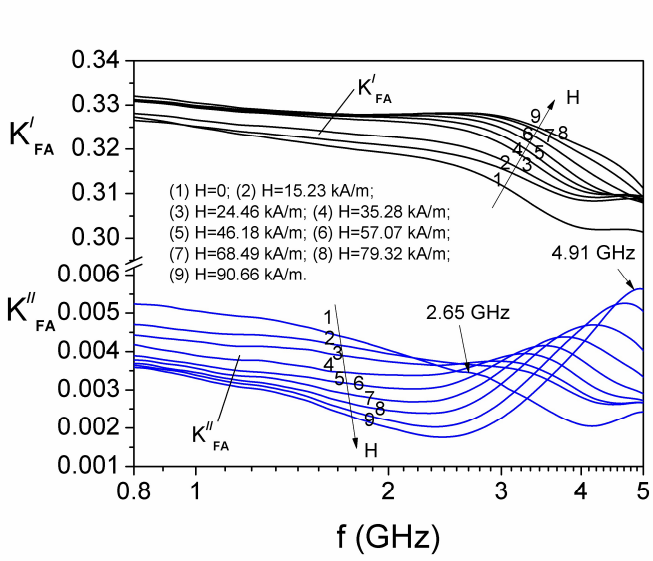

Figure 4. Frequency dependence of the components (K′FA) and (K″FA) of the Clausius-Mossotti complex factor of the ferrofluid sample in air, for different values, H, of the magnetic field.

As illustrated in Figure 4 and further detailed in Figure 5, the real part of the Clausius–Mossotti factor, K'FA, shows only a weak dependence on the applied magnetic field at frequencies up to 2 GHz. In contrast, a stronger sensitivity to the magnetic field is observed in the higher frequency range of 2 GHz – 4 GHz.

 doi:10.20944/preprints202602.1309.v1

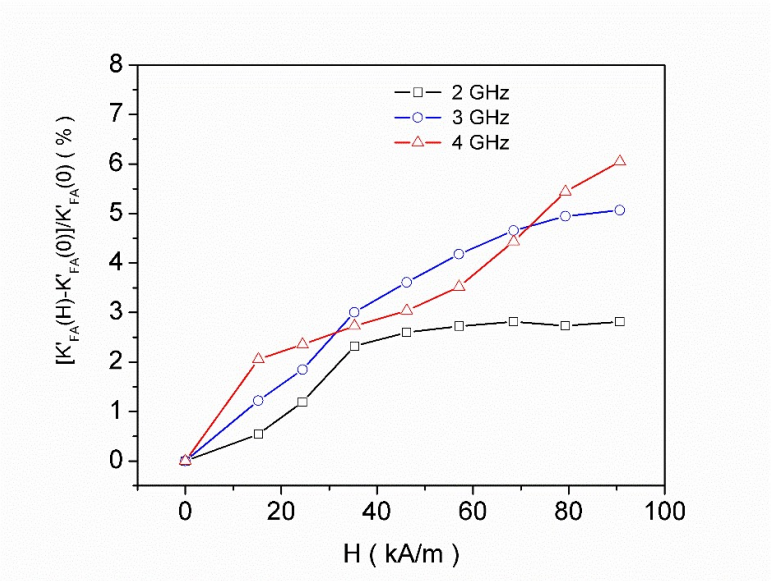

Figure 5. Relative variation of the real component of the Clausius-Mossotti factor of ferrofluid in air (K'_{FA}) as a function of the magnetic field (H).

This behavior indicates the presence of the magneto-dielectric coupling in this frequency range, which can be attributed to the magnetic-field sensitivity of the Maxwell–Wagner–Sillars relaxation process [31]. In the ferrofluid sample, this relaxation mechanism is evidenced by dielectric relaxation maxima occurring approximately within the 2 GHz – 5 GHz frequency range (see Figure 3). So, we may conclude that the presence of the magnetic field does not considerably improve the dielectrophoresis of ferrofluid droplets in air.

3.4. Clausius-Mossotti Factor of the Ferrofluid in Distilled Water

Another configuration that could be relevant for practical applications involves a mixture of water and ferrofluid droplets. To evaluate the Clausius–Mossotti factor in this case, we also measured the frequency dependence of the complex dielectric permittivity of distilled water at room temperature. Figure 6 presents this dependence over the same frequency range as that used for the ferrofluid measurements. As shown in Figure 6, the real part of the complex dielectric permittivity of water is close to 80 and decreases slightly with increasing frequency. In contrast, the imaginary part increases with frequency, approaching the characteristic maximum of distilled water, which occurs at approximately 20 GHz [32]. The magnitude of this imaginary component is therefore non-negligible and must be taken into account when calculating the Clausius–Mossotti factor for a ferrofluid droplet suspended in water.

 doi:10.20944/preprints202602.1309.v1

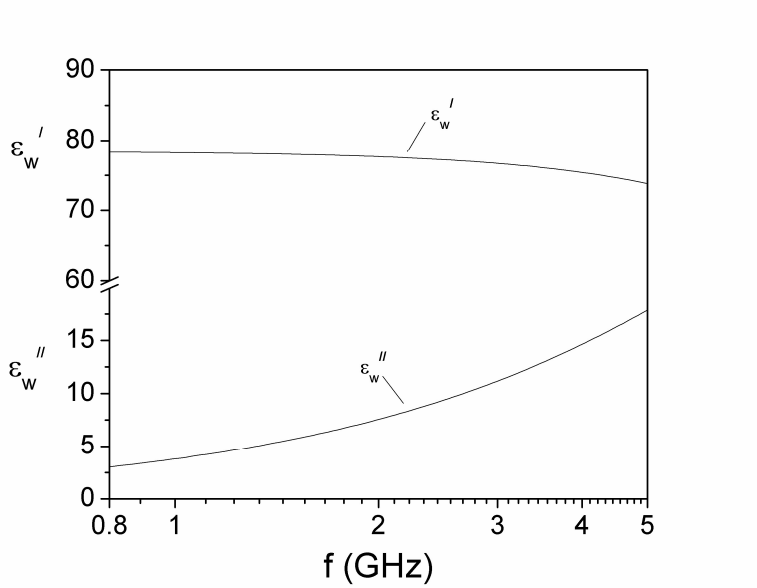

Figure 6. Frequency dependence of the components of the complex dielectric permittivity of distilled water.

The Clausius-Mossotti complex factor for a droplet of ferrofluid in distilled water is:

$$K_{FW} = \frac{\varepsilon_F^* - \varepsilon_W^*}{\varepsilon_F^* + 2\varepsilon_W^*} \tag{8}$$

Here, ε_F^* is the complex dielectric permittivity of the ferrofluid and ε_W^* is the complex dielectric permittivity of water. Using the experimental values of ε_F^* and ε_W^*, by means of equation (8), the K'FW and K''FW components of the Clausius-Mossotti complex factor of ferrofluid droplet in water were determined. Their frequency and magnetic field dependence are shown in Figure 7.

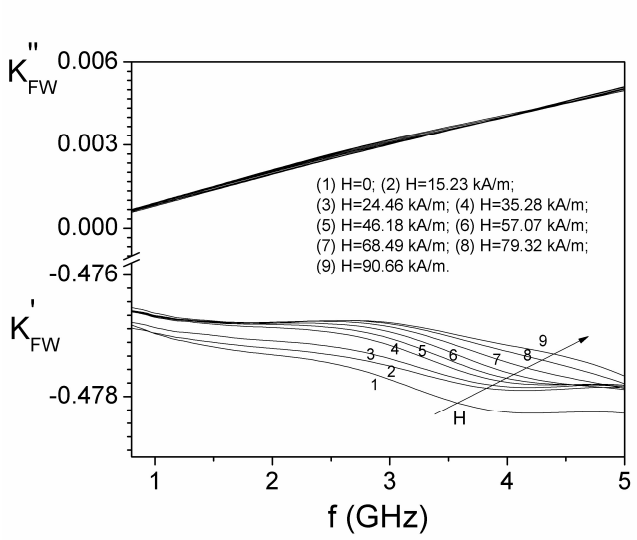

Figure 7. Frequency dependence of the components (K′FW) and (K″FW) of the Clausius-Mossotti complex factor of the ferrofluid sample in distilled water, for different values, H, of the magnetic field.

It is observed from Figure 7 that Re[KFW] is negative; therefore, the dielectrophoretic force is negative, and the ferrofluid droplet located in water is repelled from the regions of higher electric

 doi:10.20944/preprints202602.1309.v1

field intensity. With respect to the influence of the magnetic field on the components of the Clausius–Mossotti factor, Figure 7 demonstrates that neither the real part, K'_{FW}, nor the imaginary part, K''_{FW}, exhibits a significant dependence on the applied magnetic field, H. This behavior can be attributed to the substantially higher permittivity of water relative to that of the ferrofluid. As a result, the Clausius–Mossotti factor for a ferrofluid dispersed in water is predominantly governed by the permittivity of the surrounding water medium, which is essentially insensitive to variations in the magnetic field.

3.5. Proving the Existence of Dielectrophoretic Force in the Microwave Field

To demonstrate the presence of dielectrophoretic forces in the microwave frequency range, we conducted a qualitative experiment using a quarter-wavelength ($\lambda/4$) antenna connected to a network analyzer via a 50 Ω coaxial cable. Figures 8(a) and 8(b) show the experimental setup and a detailed view of the antenna, respectively. For a quarter-wavelength ($\lambda/4$) antenna, the electric field reaches its maximum at the antenna tip. To further enhance the electric field intensity, a thin wire with a diameter of 150 μm was soldered to the end of the antenna (see Figure 8 (b)). The total length of the antenna was 5 cm. In order to find the tuning frequency of the cable-antenna system, we measured the frequency dependence of the S11 parameter, and the result is shown in Figure 9, from which it can be seen that the tuning frequency is at 1.66 GHz.

a) (**b**)

Figure 8. Pictures of the experimental arrangement for proving the microwave dielectrophoresis force: general view (**a**) and details with the antenna and pendulum (**b**).

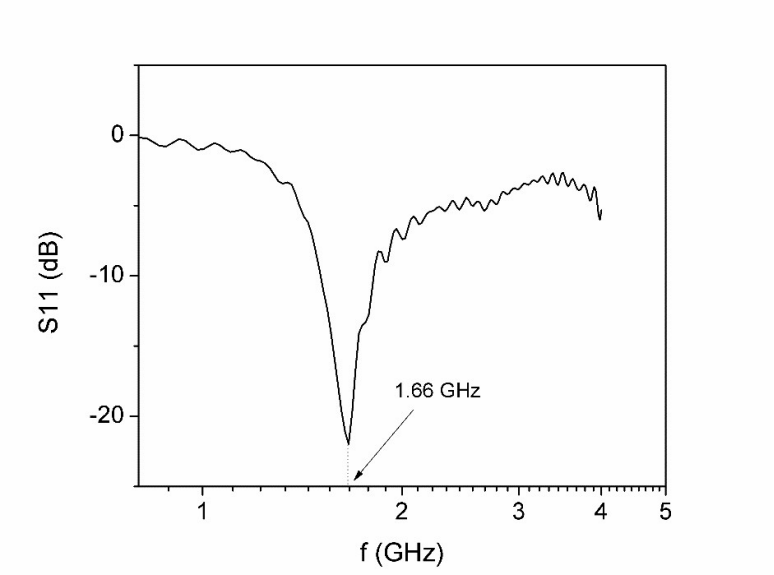

 doi:10.20944/preprints202602.1309.v1

Figure 9. Frequency dependence of the reflection coefficient of the cable-antenna system.

At the frequency corresponding to the minimum of the reflection coefficient (S11), the antenna operates in resonant mode. In this case, the electromagnetic field distribution along a $\lambda/4$ antenna exhibits a maximum of the electric field at the free end of the antenna. Since the network analyzer performs measurements over a user-defined frequency range, and taking into account the resonant frequency of the cable–antenna system, the scan range was narrowed to (1.6 – 1.7) GHz, in order to emphasize the dielectrophoretic force in the vicinity of the resonance.

Near the free end of the antenna, a pendulum consisting of a textile thread was positioned (see Figure 8(b)). The lower end of the thread was first immersed in the ferrofluid and subsequently brought close to the antenna tip together with its support, until the thread adhered to the antenna end. The support was then carefully withdrawn, while ensuring that the thread remained attached to the antenna. The support was further displaced until the thread detached from the antenna tip. After allowing the thread to reach its equilibrium position, the horizontal displacement between the thread and the antenna tip was measured as d = 0.5 cm (see Figure 10).

Figure 10. Frequency dependence of the reflection coefficient of the cable-antenna system.

Given the thread length, L = 12 cm, and its mass, m = 19 mg, the horizontal force—attributed to the dielectrophoretic effect—required to balance the gravitational force and maintain the thread end at a horizontal displacement, d, from the vertical was estimated to be $F = 3.9 \cdot 10^{-6}$ N.

4. Conclusions

The real, ε'_F and imaginary, ε''_F components of the complex dielectric permittivity, over the frequency range (0.8 – 5) GHz and at different values of a static magnetic field, H, between approximately (0-91) kA/m, for a kerosene-based ferrofluid sample, with Mn-Fe nanoparticles, were determined. The results show that ε''_F has a maximum at a frequency f_{max} that increases from 2.65 GHz to 4.70 GHz with increasing H from 0 to 90.66 kA/m, indicating the presence of a magnetic field-dependent dielectric relaxation process, associated with the Maxwell-Wagner-Sillars polarization phenomenon, or interfacial polarization.

We investigated the feasibility of extracting nanoparticles from ferrofluids via dielectrophoresis by analyzing the squared electric field gradient (∇E^2). For gradients below the threshold of $(\nabla E^2)_{min}$, the dielectrophoretic force is weaker than the Brownian force. Consequently, under these conditions, and in the absence of additional factors that might induce local nanoparticle aggregation, the ferrofluid can be considered a homogeneous dielectric from the dielectrophoretic point of view.

Based on the ε'_F and ε''_F components of the complex dielectric permittivity of the ferrofluid, and the components of the complex dielectric permittivity of distilled water, the effect of the magnetic field, H, on the Clausius-Mossotti complex factor, K*(f, H), at different microwave frequencies was analyzed, for two cases: ferrofluid droplets in air and ferrofluid droplets in distilled water.

 doi:10.20944/preprints202602.1309.v1

In air, the Clausius-Mossotti factor shows a modest yet reliable dependence on the magnetic field, reflecting a magnetically modulated dielectric response at GHz frequencies. By contrast, when water serves as the reference medium, the Clausius-Mossotti factor remains negative and largely unaffected by H across the studied frequency range, indicating that water's high permittivity suppresses the magneto-dielectric effect of ferrofluids.

Using a $\lambda/4$ antenna connected to a network analyzer, the resonant frequency of the cable-antenna system was determined. Around this resonant frequency, the dielectrophoretic force acting on the end of a textile thread, after it was immersed in ferrofluid, was evaluated. This demonstrates the existence of the dielectrophoretic force at microwave frequencies.

Author Contributions: Conceptualization, C.N.M. and I.M.; methodology, X.X.; software, X.X.; validation, C.N.M, I.M. and C.F.M.; formal analysis, I.M. and C.F.M.; investigation, C.N.M and P.C.F; resources, C.N.M.; data curation, I.M.; writing—original draft preparation, I.M. and C.N.M.; writing—review and editing, I.M., C.F.M. and C.N.M.; visualization, X.X.; supervision, C.N.M. All authors have read and agreed to the published version of the manuscript.

Funding: This research was funded by UEFISCDI, grant number 12CoEx/2026 (acronym – ARMAT - Center of Excellence for Advanced Responsive Materials).

Data Availability Statement: The data presented in this study are available on request from the corresponding author.

Acknowledgments: The authors acknowledge the support given by the institutions where they are employed.

Conflicts of Interest: The authors declare no conflicts of interest.

Abbreviations

The following abbreviations are used in this manuscript:

CM	Clausius-Mossotti factor
DEP	Dielectrophoresis
OC	Open-circuited coaxial transmission line technique

References

1. Rosensweig, R.E. *Ferrohydrodynamics*; Cambridge University Press: Cambridge, UK, 1985.
2. Charles, S.W. The preparation of magnetic fluids. In *Ferrofluids, Magnetically Controllable Fluids and Their Applications*; Odenbach, S., Ed.; Springer: Berlin/Heidelberg, Germany, 2002; Volume 524, pp. 3–18.
3. Scherer, C.; Figueiredo Neto, A.M. Ferrofluids: Properties and applications. *Braz. J. Phys.* **2005**, *35*, 718–727.
4. Kole, M.; Khandekar, S. Engineering applications of ferrofluids: A review. *J. Magn. Magn. Mater.* **2021**, *537*, 168222.
5. Mehta, M.; Bhandari, A. Advancement in biomedical applications of ferrofluids. *J. Braz. Soc. Mech. Sci. Eng.* **2025**, *47*, 490.
6. Minuti, A.E.; Stoian, G.; Herea, D.-D.; Radu, E.; Lupu, N.; Chiriac, H. Fe–Cr–Nb–B ferrofluid for biomedical applications. *Nanomaterials* **2022**, *12*, 1488.
7. Kirby, B.J. *Micro- and Nanoscale Fluid Mechanics: Transport in Microfluidic Devices*; Cambridge University Press: Cambridge, UK, 2010; ISBN 978-0-521-11903-0.
8. Zhang, H.; Chang, H.; Neuzil, P. DEP-on-a-Chip: Dielectrophoresis Applied to Microfluidic Platforms. *Micromachines* **2019**, *10*, 423. https://doi.org/10.3390/mi10060423.
9. Pesch, G.R.; Du, F. A review of dielectrophoretic separation and classification of non-biological particles. *Electrophoresis* **2021**, *42*, 134–152. https://doi.org/10.1002/elps.202000137.
10. Luo, X.; Wu, C.; Zhang, J.; Xu, J.; Tan, H.; Zhang, B.; Xie, J.; Tao, C.; Huang, K.; Cheng, X.; Wen, W. Direct dielectrophoretic characterization of particles in the high-density microwell array using optical tweezers. *Opt. Lasers Eng.* **2024**, *174*, 107976. https://doi.org/10.1016/j.optlaseng.2023.107976.

 doi:10.20944/preprints202602.1309.v1

11. Abd Rahman, N.; Ibrahim, F.; Yafouz, B. Dielectrophoresis for Biomedical Sciences Applications: A Review. Sensors **2017**, *17*, 449. https://doi.org/10.3390/s17030449.
12. Lagally, E.T.; Lee, S.-H.; Soh, H.T. Integrated microsystem for dielectrophoretic cell concentration and genetic detection. *Lab Chip* **2005**, *5*, 1053–1058. https://doi.org/10.1039/B505915A.
13. Asami, K. Low-frequency dielectric dispersion of bacterial cell suspensions. *Colloids Surf. B Biointerfaces* **2014**, *119*, 1–5. https://doi.org/10.1016/j.colsurfb.2014.04.014.
14. Alshareef, M.; Metrakos, N.; Juarez Perez, E.; Azer, F.; Yang, F.; Yang, X.; Wang, G. Separation of tumor cells with dielectrophoresis-based microfluidic chip. *Biomicrofluidics* **2013**, *7*, 011803. https://doi.org/10.1063/1.4774312.
15. Chung, C.; Pethig, R.; Smith, S.; Waterfall, M. Intracellular potassium under osmotic stress determines the dielectrophoresis cross-over frequency of murine myeloma cells in the MHz range. *Electrophoresis* **2018**, *39*, 989–997. https://doi.org/10.1002/elps.201700433.
16. Secme, A.; Kucukoglu, B.; Pisheh, H.S.; Alatas, Y.C.; Tefek, U.; Uslu, H.D.; Kaynak, B.E.; Alhmoud, H.; Hanay, M.S. Dielectric detection of single nanoparticles using a microwave resonator integrated with a nanopore. *ACS Omega* **2024**, *9*, 7827–7834. https://doi.org/10.1021/acsomega.3c07506.
17. Afshar, S.; Salimi, E.; Braasch, K.; Butler, M.; Thomson, D.J.; Bridges, G.E. Multi-frequency DEP cytometer employing a microwave sensor for dielectric analysis of single cells. *IEEE Trans. Microw. Theory Tech.* **2016**, *64*, 991–998. https://doi.org/10.1109/TMTT.2016.2518178.
18. Mun, P.S.; Ting, H.N.; Ong, T.A.; Wong, C.M.; Ng, K.H. A study of dielectric properties of proteinuria between 0.2 GHz and 50 GHz. *PLoS ONE* **2015**, *10*, e0130011. https://doi.org/10.1371/journal.pone.0130011.
19. Gabor, L.; Minea, R.; Gabor, D. Magnetic Liquids Filtering Process. RO Patent 108851, 30 September 1994.
20. Malaescu, I.; Gabor, L.; Claici, F.; Stefu, N. Study of some magnetic properties of ferrofluids filtered in magnetic field gradient. *J. Magn. Magn. Mater.* **2000**, *222*, 8–12.
21. Daniela Susan-Resiga, I. Malaescu, Oana Marinica, C.N. Marin, Magnetorheological properties of a kerosene-based ferrofluid with magnetite particles hydrophobized in the absence of the dispersion medium, *Physica B* **2020**, *587* 412150.
22. Ercuta, A. Sensitive AC hysteresigraph of extended driving field capability. *IEEE Trans. Instrum. Meas.* **2020**, *69*, 1643–1651.
23. Chantrell, R.W.; Popplewell, J.; Charles, S.W. Measurements of particle size distribution parameters in ferrofluids. *IEEE Trans. Magn.* **1978**, *14*, 975–977.
24. Fannin, P.C. Use of Ferromagnetic Resonance Measurements in Magnetic Fluids. *J. Mol. Liquids* **2004**, *114*, 79–87.
25. Fannin, P.C.; MacOireachtaigh, C.; Couper, C. An Improved Technique for the Measurement of the Complex Susceptibility of Magnetic Colloids in the Microwave Region. *J. Magn. Magn. Mater.* **2010**, *322*, 2428–2433.
26. Kurnia, A.; Heriansyah, A.; Suharyadi, E. Study on the Influence of Crystal Structure and Grain Size on Dielectric Properties of Manganese Ferrite ($MnFe_2O_4$) Nanoparticles. *IOP Conf. Ser. Mater. Sci. Eng.* **2017**, *202*, 012046. https://doi.org/10.1088/1757-899X/202/1/012046.
27. Asbury, C.L.; Diercks, A.H.; van den Engh, G. Trapping of DNA by dielectrophoresis. *Electrophoresis* **2002**, *23*, 2658–2666. https://doi.org/10.1002/1522-2683(200208)23:16.
28. Cully, J.J.; Swett, J.L.; Willick, K.; Baugh, J.; Mol, J.A. Graphene nanogaps for the directed assembly of single-nanoparticle devices. *Nanoscale* **2021**, *13*, 6513–6520. https://doi.org/10.1039/D1NR01450A.
29. McMullen, R.; Mishra, A.; Slinker, J.D. Straightforward Fabrication of Sub-10 nm Nanogap Electrode Pairs by Electron Beam Lithography. *Precision Engineering* **2022**, *77*, 275–280. https://doi.org/10.1016/j.precisioneng.2022.06.004.
30. Samet, M.; Kallel, A.; Serghei, A. Maxwell-Wagner-Sillars interfacial polarization in dielectric spectra of composite materials: Scaling laws and applications. *J. Comp. Mater.* **2022**, *56*, 3197–3217.
31. Marin, C.N.; Fannin, P.C.; Raj, K.; Socoliuc, V. Magnetodielectric spectroscopy of magnetic fluids. *Magnetohydrodynamics* **2013**, *49*, 270–276.
32. Kaatze, U. Complex permittivity of water as a function of frequency and temperature. *J. Chem. Eng. Data* **1989**, *34*, 371–374. https://doi.org/10.1021/je00058a001

 doi:10.20944/preprints202602.1309.v1